Fully self-consistent mean-field model of asymmetric nuclear matter*

K. Miyazaki

Abstract

We have developed a new relativistic mean-field model of asymmetric nuclear matter. It is an extension of the Zimanyi-Moszkowski model based on the constituent quark picture of nucleons. The effects of the scalar mean-fields on all the three constituent quarks in medium have been taken into account. They produce the renormalized effective coupling constants to be dependent on the effective masses of nucleons. Including the isovector scalar mean-field by $\delta[a_0(980)]$ meson, the masses of protons and neutrons are different from each other. Consequently, we have charge-asymmetric effective interactions to be determined self-consistently as well as the effective masses. We have numerically investigated the charge-asymmetric nature of our model in detail. Then it is applied to the cold β-stable neutron stars. The results exhibit the general feature of a stiff equation-of-state.

1 Introduction

There are growing interests on asymmetric hadronic matter at high density in the relation to high-energy heavy-ion collisions and astrophysics. Theoretically, the high-density matter should be described within a relativistic framework. A lot of investigations have been performed based on the relativistic mean-field theory as the so-called Walecka model [1] or its nonlinear extension (NLW). However they are not consistent in the following respect.

The nucleon in the relativistic mean-fields is not a physically observed nucleon but a quasi-particle or dressed nucleon. Therefore the interactions between two nucleons mediated by various mesons are the effective ones. In asymmetric matter, the effective interactions are not necessary to be charge symmetric or invariant. This is theoretically realized in the Dirac-Brueckner-Hartree-Fock (DBHF) model [2-4]. (Precisely, this is also realized in the nonrelativistic Brueckner-Hartree-Fock model.) The three G-matrices describing proton-proton, neutron-neutron and proton-neutron scattering are different from each other in asymmetric medium. However, neither the Walecka nor the NLW model can take into account the charge asymmetry of the effective interactions. Moreover, the phenomenological effective mean-field models [4-6] of the DBHF theory do not treat

*This paper is the revised version of CDS ext-2003-077. A few mistakes as well as some texts and mistypes have been corrected.

the asymmetry explicitly since their meson-nucleon coupling constants are determined from numerical results of the nucleon self-energies by the DBHF calculation [7].

We have seen that the fully self-consistent theory of asymmetric matter should deal with the charge asymmetry of the densities, effective masses and effective interactions of protons and neutrons, simultaneously. Until now there have been no relativistic mean-field models to satisfy such a condition. We can however find a promising candidate, that is, the derivative scalar-coupling model developed by Zimanyi and Moszkowski (ZM) [8]. This model gives the renormalized $NN\sigma$ coupling constant $g^*_{NN\sigma} = (M^*_N/M_{_N})\, g_{NN\sigma}$ where $g_{NN\sigma}$ is the phenomenological $NN\sigma$ coupling constant determined to reproduce the nuclear matter saturation. M_N is the free mass of a nucleon and M^*_N is its effective mass in the medium. If the effective masses of protons M^*_p and neutrons M^*_n are different in asymmetric matter [9,10], we have the charge asymmetry of the coupling constant $g^*_{pp\sigma} \neq g^*_{nn\sigma}$. Of course, this simple discussion is not sufficient. We have to consider the isoscalar mesons σ and ω as well as isovector mesons $\delta[a_0(980)]$ and ρ in a fully self-consistent method.

However the straightforward extensions of the ZM model to asymmetric matter in Refs. [11,12] are not suitable to our purpose. They applied the renormalization factor $g^*_{NN\sigma}/g_{NN\sigma} = (1 + g_{NN\sigma}\,\langle\sigma\rangle/M_{_N})^{-1}$ to all the meson-nucleon couplings, where $\langle\sigma\rangle$ is the mean field of the σ meson. In this case, the renormalized (or effective) coupling constants are determined by only the isoscalar mean field. Therefore the charge asymmetry of the effective interactions cannot be realized.

Recently, another interpretation and extension of the ZM model [13] has been developed to describe charge-symmetric strange hadronic matter based on the constituent quark picture of baryons. This model remedies the deficiency of the original ZM model that cannot reproduce the strong spin-orbit potential, and produces the similar properties of symmetric nuclear matter to the DBHF calculation. The purpose of the present work is a generalization of the model in Ref. [13] to asymmetric nuclear matter. We will find that it can describe the charge asymmetry in a fully consistent manner. The detailed formulation of the model is given in the next section. The numerical results of asymmetric matter are shown in section 3. Especially, the charge asymmetries of the effective interactions or the meson-nucleon coupling constants are investigated in detail. Furthermore the model will be applied to neutron stars. Finally, we summarize our investigations and draw conclusions in section 4.

2 Generalization of the ZM model to asymmetric matter

Here the renormalized effective coupling constants in asymmetric matter are derived based on the method developed in Ref. [13]. Then they are used to construct the mean-field

model. We consider the contributions by the isoscalar scalar meson σ, isoscalar vector meson ω and isovector vector meson ρ. Furthermore the isovector scalar meson $\delta[a_0(980)]$ is introduced to produce the different effective masses of protons and neutrons [9,10]. In this work, the same free masses for proton and neutron, $M_p = M_n = M_N$, are assumed, and the electro-magnetic interactions are not considered.

2.1 Renormalized coupling constants

We first consider $pp\sigma$ and $pp\omega$ couplings. In the constituent quark picture of a proton (p), unrenormalized free coupling constant $g_{pp\sigma(\omega)}$ is schematically written as

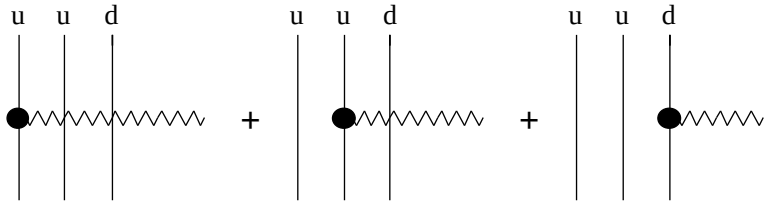

or expressed by

$$g_{pp\,\sigma(\omega)} = 3\, g_{qq\sigma(\omega)}, \tag{1}$$

where q denotes u or d quark. Equation (1) is also valid for a neutron (n). Thus

$$g_{NN\sigma(\omega)} = g_{pp\,\sigma(\omega)} = g_{nn\sigma(\omega)} = 3\, g_{qq\,\sigma(\omega)}. \tag{2}$$

Here the two quarks in a nucleon are the spectators or free constituents. However all the three quarks in a nuclear nucleon are embedded in the medium. This fact should produce the medium correction to $g_{NN\sigma(\omega)}$. It was investigated in Ref. [13] for symmetric matter and the effective coupling constants being similar to but more reasonable than those in the ZM model were obtained.

Extension of the model in Ref. [13] to asymmetric matter is straightforward. It is only noted that the scalar mean-fields of u and d quarks are different from each other. Then we have the following medium correction term to $g_{pp\sigma(\omega)}$.

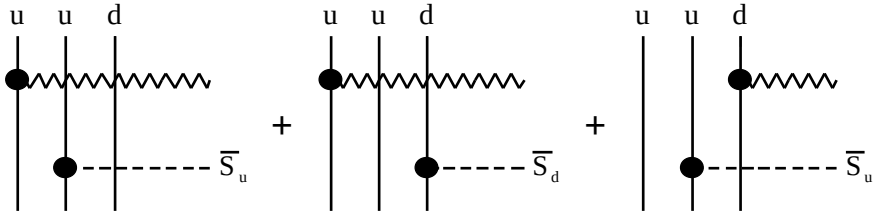

where the wavy lines are σ or ω mesons. The dashed lines are the effects of the mean-fields of quarks defined by

$$\bar{S}_{u(d)} \equiv S_{u(d)}/M_N. \tag{3}$$

where S_u and S_d are the scalar potentials of u and d quarks. Adding the above correction to Eq. (1), we have the renormalized effective $pp\sigma(\omega)$ coupling constant $g^*_{pp\sigma(\omega)}$,

$$\begin{aligned} g^*_{pp\sigma(\omega)} &= g_{NN\sigma(\omega)} + \left(2\bar{S}_u + \bar{S}_d\right) g_{qq\sigma(\omega)} = \left[1 + \frac{1}{3}\left(2\bar{S}_u + \bar{S}_d\right)\right] g_{NN\sigma(\omega)}, \\ &= \left(1 + \frac{1}{3}\bar{S}_p\right) g_{NN\sigma(\omega)} = \left[(1-\lambda_N) + \lambda_N m^*_p\right] g_{NN\sigma(\omega)}, \end{aligned} \tag{4}$$

where S_p is the scalar potential of protons

$$\bar{S}_p \equiv S_p/M_N = 2\bar{S}_u + \bar{S}_d, \tag{5}$$

and

$$m^*_p \equiv M^*_p/M_N = \left(M_N + S_p\right)/M_N, \tag{6}$$

$$\lambda_N = 1/3. \tag{7}$$

Similarly, the renormalized effective $nn\sigma(\omega)$ coupling constant $g^*_{nn\sigma(\omega)}$ is

$$\begin{aligned} g^*_{nn\sigma(\omega)} &= g_{NN\sigma(\omega)} + \left(\bar{S}_u + 2\bar{S}_d\right) g_{qq\sigma(\omega)} = \left[1 + \frac{1}{3}\left(\bar{S}_u + 2\bar{S}_d\right)\right] g_{NN\sigma(\omega)}, \\ &= \left(1 + \frac{1}{3}\bar{S}_n\right) g_{NN\sigma(\omega)} = \left[(1-\lambda_N) + \lambda_N m^*_n\right] g_{NN\sigma(\omega)}, \end{aligned} \tag{8}$$

where S_n is the scalar potential of neutrons

$$\bar{S}_n \equiv S_n/M_N = \bar{S}_u + 2\bar{S}_d\,, \tag{9}$$

and

$$m^*_n \equiv M^*_n/M_N = \left(M_N + S_n\right)/M_N. \tag{10}$$

Essential difference between the present results and Ref. [13] is that the values of $\bar{S}_u$ and $\bar{S}_d$ or m^*_p and m^*_n are different;

$$\bar{S}_u \neq \bar{S}_d\,, \tag{11}$$

$$m^*_p \neq m^*_n. \tag{12}$$

As a result the $NN\sigma(\omega)$ coupling becomes charge asymmetric,

$$g^*_{pp\sigma(\omega)} \neq g^*_{nn\sigma(\omega)}. \tag{13}$$

If $m^*_p = m^*_n = m^*_N$, we have the same results as Ref. [13]. Furthermore, in the case of

$\lambda_N = 1$, the ZM model is recovered.

Equations (11) and (12) are due to the contribution by the isovector scalar mean-filed. Then we consider the isovector mesons $\delta[a_0(980)]$ and ρ. In the constituent quark picture of a proton, unrenormalized free $NN\delta$ or $NN\rho$ coupling constant is expressed by

$$g_{pp\,\delta(\rho)} = g_{nn\delta(\rho)} = g_{NN\,\delta(\rho)} = g_{qq\delta(\rho)}. \tag{14}$$

According to the same procedure as the isoscalar mesons, the medium correction to $pp\delta(\rho)$ coupling constant is schematically written by

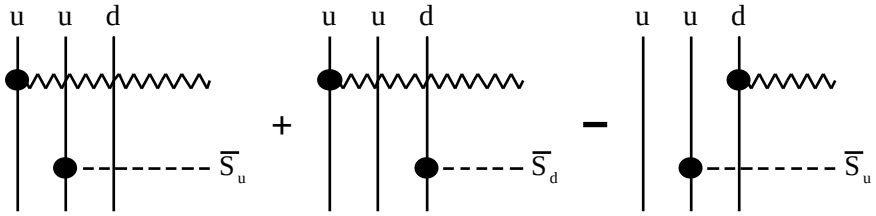

where the wavy lines are δ or ρ mesons. Thus, the renormalized effective $pp\delta(\rho)$ coupling constant $g^*_{pp\delta(\rho)}$ is

$$\begin{aligned} g^*_{pp\,\delta(\rho)} &= g_{NN\delta(\rho)} + \bar{S}_d\, g_{qq\delta(\rho)} = \left(1 + \bar{S}_d\right) g_{NN\delta(\rho)}, \\ &= \left[(1-\lambda_N) + \lambda_N \left(2m^*_n - m^*_p\right)\right] g_{NN\delta(\rho)}. \end{aligned} \tag{15}$$

Similarly, the renormalized effective $nn\delta(\rho)$ coupling constant $g^*_{nn\delta(\rho)}$ is

$$\begin{aligned} g^*_{nn\delta(\rho)} &= g_{NN\delta(\rho)} + \bar{S}_u\, g_{qq\delta(\rho)} = \left(1 + \bar{S}_u\right) g_{NN\delta(\rho)}, \\ &= \left[(1-\lambda_N) + \lambda_N \left(2m^*_p - m^*_n\right)\right] g_{NN\delta(\rho)}. \end{aligned} \tag{16}$$

We have also the charge asymmetry,

$$g^*_{pp\,\delta(\rho)} \neq g^*_{nn\delta(\rho)}. \tag{17}$$

Consequently, the model developed in Ref. [13] can be extended straightforwardly to asymmetric matter and reproduce the charge-asymmetric effective interactions between two nucleons in medium as the DBHF theory does. Our intuitive method may arise some suspicion about its theoretical foundation. However, in the symmetric case $m^*_p = m^*_n$, almost the same effective coupling constant as Eq. (4) or (8) has been derived in the renormalized Walecka model of Ref. [14], which takes into account the effect of meson cloud surrounding the nucleons in medium.

2.2 The mean-filed model of asymmetric matter

Using the renormalized effective meson-nucleon coupling constants obtained above, our mean-field model Lagrangian for asymmetric nuclear matter becomes

$$\begin{aligned}\mathcal{L} &= \bar{\psi}_p \left(\not{p} - M_p^* - \gamma^0 V_p \right) \psi_p + \bar{\psi}_n \left(\not{p} - M_n^* - \gamma^0 V_n \right) \psi_n \\ &\quad - \frac{1}{2} m_\sigma^2 \langle \sigma \rangle^2 + \frac{1}{2} m_\omega^2 \langle \omega_0 \rangle^2 - \frac{1}{2} m_\delta^2 \langle \delta_3 \rangle^2 + \frac{1}{2} m_\rho^2 \langle \rho_{03} \rangle^2 . \end{aligned} \tag{18}$$

where ψ_p and ψ_n are the Dirac fields of protons and neutrons, $\langle \sigma \rangle$, $\langle \omega_0 \rangle$, $\langle \delta_3 \rangle$ and $\langle \rho_{03} \rangle$ are the mean-fields and m_σ, m_ω, m_δ and m_ρ are the masses of each meson. The scalar and vector potentials are given by

$$S_p = -g^*_{pp\,\sigma} \langle \sigma \rangle - g^*_{pp\,\delta} \langle \delta_3 \rangle , \tag{19}$$

$$S_n = -g^*_{nn\sigma} \langle \sigma \rangle + g^*_{nn\delta} \langle \delta_3 \rangle , \tag{20}$$

$$V_p = g^*_{pp\,\omega} \langle \omega_0 \rangle + g^*_{pp\rho} \langle \rho_{03} \rangle , \tag{21}$$

$$V_n = g^*_{nn\omega} \langle \omega_0 \rangle - g^*_{nn\rho} \langle \rho_{03} \rangle . \tag{22}$$

From Eqs. (19)-(22), the meson mean-fields are inversely expressed by the potentials. Therefore the energy density is written by

$$\begin{aligned}\mathcal{E} &= \left(\langle E_k^* \rangle_p + V_p \right) \rho_{pB} + \left(\langle E_k^* \rangle_n + V_n \right) \rho_{nB} \\ &\quad + \frac{1}{2} m_\sigma^2 \left[\frac{g^*_{nn\delta} \left(M_p^* - M_p \right) + g^*_{pp\delta} \left(M_n^* - M_n \right)}{g^*_{pp\,\sigma}\, g^*_{nn\delta} + g^*_{nn\sigma}\, g^*_{pp\delta}} \right]^2 \\ &\quad + \frac{1}{2} m_\delta^2 \left[\frac{g^*_{nn\sigma} \left(M_p^* - M_p \right) - g^*_{pp\sigma} \left(M_n^* - M_n \right)}{g^*_{pp\sigma}\, g^*_{nn\delta} + g^*_{nn\sigma}\, g^*_{pp\delta}} \right]^2 \\ &\quad - \frac{1}{2} m_\omega^2 \left(\frac{g^*_{nn\rho} V_p + g^*_{pp\rho} V_n}{g^*_{pp\,\omega}\, g^*_{nn\rho} + g^*_{nn\omega}\, g^*_{pp\rho}} \right)^2 - \frac{1}{2} m_\rho^2 \left(\frac{g^*_{nn\omega} V_p - g^*_{pp\,\omega} V_n}{g^*_{pp\,\omega}\, g^*_{nn\rho} + g^*_{nn\omega}\, g^*_{pp\rho}} \right)^2 , \end{aligned} \tag{23}$$

where $\langle E_k^* \rangle_{p(n)}$ is the average kinetic energy and $\rho_{p(n)B}$ is the baryon density of protons (neutrons). The vector potentials are determined by $\partial \mathcal{E} / \partial V_p = 0$ and $\partial \mathcal{E} / \partial V_n = 0$. Then we have

$$V_p = \left(\frac{{g^*_{pp\,\omega}}^2}{m_\omega^2} + \frac{{g^*_{ppp}}^2}{m_\rho^2} \right) \rho_{pB} + \left(\frac{g^*_{pp\,\omega}\, g^*_{nn\omega}}{m_\omega^2} - \frac{g^*_{pp\rho}\, g^*_{nn\rho}}{m_\rho^2} \right) \rho_{nB}, \tag{24}$$

$$V_n = \left(\frac{{g^*_{nn\omega}}^2}{m_\omega^2} + \frac{{g^*_{nn\rho}}^2}{m_\rho^2} \right) \rho_{nB} + \left(\frac{g^*_{pp\,\omega}\, g^*_{nn\omega}}{m_\omega^2} - \frac{g^*_{pp\rho}\, g^*_{nn\rho}}{m_\rho^2} \right) \rho_{pB}. \tag{25}$$

Substituting Eqs. (24) and (25), the energy density becomes

$$\begin{aligned}\mathcal{E} &= f_p \langle E_k^* \rangle_p \rho_T + f_n \langle E_k^* \rangle_n \rho_T + \frac{1}{2} M_N^2 \left(\frac{m_\sigma}{g_{NN\sigma}}\right)^2 \left[\frac{h^*_{nn\delta}\left(m_p^*-1\right)+h^*_{pp\delta}\left(m_n^*-1\right)}{h^*_{pp\sigma}h^*_{nn\delta}+h^*_{nn\sigma}h^*_{pp\delta}}\right]^2 \\ &+ \frac{1}{2} M_N^2 \left(\frac{m_\delta}{g_{NN\delta}}\right)^2 \left[\frac{h^*_{nn\sigma}\left(m_p^*-1\right)-h^*_{pp\sigma}\left(m_n^*-1\right)}{h^*_{pp\sigma}h^*_{nn\delta}+h^*_{nn\sigma}h^*_{pp\delta}}\right]^2 \\ &+ \frac{1}{2}\left(\frac{g_{NN\omega}}{m_\omega}\right)^2 \left(f_p\, h^*_{pp\,\omega}+f_n\, h^*_{nn\omega}\right)^2 \rho_T^2 + \frac{1}{2}\left(\frac{g_{NN\rho}}{m_\rho}\right)^2 \left(f_p\, h^*_{pp\rho}-f_n\, h^*_{nn\rho}\right)^2 \rho_T^2, \end{aligned} \tag{26}$$

where we have used the total baryon density $\rho_T = \rho_{pB} + \rho_{nB}$ and the proton (neutron) fraction $f_{p(n)}$, and Eqs. (4), (8), (15) and (16) are abbreviated as

$$g^*_{pp(nn)M} = h^*_{pp(nn)M}\, g_{NNM} \quad (M = \sigma,\ \omega,\ \delta,\ \rho)\,. \tag{27}$$

The effective masses m_p^* and m_n^* are determined by solving the self-consistency equations $\partial\mathcal{E}/\partial m_p^* = 0$ and $\partial\mathcal{E}/\partial m_n^* = 0$ simultaneously. From Eq. (26), we have

$$\begin{aligned} & f_p \frac{\rho_{pS}}{\rho_{pB}} + \frac{A^{(0)}\left(A_p^{(1)}C^{(0)}-A^{(0)}C_p^{(1)}\right)}{\left(C^{(0)}\right)^3}\left(\frac{m_\sigma}{g_{NN\sigma}}\right)^2 \frac{M_N}{\rho_T} \\ & + \frac{B^{(0)}\left(C^{(0)}-B^{(0)}C_p^{(1)}\right)}{\left(C^{(0)}\right)^3}\left(\frac{m_\delta}{g_{NN\delta}}\right)^2 \frac{M_N}{\rho_T} + \lambda_N f_p \left(f_p\, h^*_{pp\,\omega}+f_n\, h^*_{nn\omega}\right)\left(\frac{g_{NN\omega}}{m_\omega}\right)^2 \frac{\rho_T}{M_N} \\ & - \lambda_N \left(f_p+2f_n\right)\left(f_p\, h^*_{pp\rho}-f_n\, h^*_{nn\rho}\right)\left(\frac{g_{NN\rho}}{m_\rho}\right)^2 \frac{\rho_T}{M_N} = 0, \end{aligned} \tag{28}$$

$$\begin{aligned} & f_n \frac{\rho_{nS}}{\rho_{nB}} + \frac{A^{(0)}\left(A_n^{(1)}C^{(0)}-A^{(0)}C_n^{(1)}\right)}{\left(C^{(0)}\right)^3}\left(\frac{m_\sigma}{g_{NN\sigma}}\right)^2 \frac{M_N}{\rho_T} \\ & - \frac{B^{(0)}\left(C^{(0)}+B^{(0)}C_n^{(1)}\right)}{\left(C^{(0)}\right)^3}\left(\frac{m_\delta}{g_{NN\delta}}\right)^2 \frac{M_N}{\rho_T} + \lambda_N f_n \left(f_p\, h^*_{pp\,\omega}+f_n\, h^*_{nn\omega}\right)\left(\frac{g_{NN\omega}}{m_\omega}\right)^2 \frac{\rho_T}{M_N} \\ & + \lambda_N \left(2f_p+f_n\right)\left(f_p\, h^*_{pp\rho}-f_n\, h^*_{nn\rho}\right)\left(\frac{g_{NN\rho}}{m_\rho}\right)^2 \frac{\rho_T}{M_N} = 0, \end{aligned} \tag{29}$$

where $\rho_{p(n)S}$ is the scalar density of protons (neutrons). The quantities A, B and C are defined by

$$A^{(0)} = h^*_{nn\delta}\left(m_p^*-1\right)+h^*_{pp\delta}\left(m_n^*-1\right), \tag{30}$$

$$B^{(0)} = h^*_{nn\sigma}\left(m_p^*-1\right)-h^*_{pp\sigma}\left(m_n^*-1\right), \tag{31}$$

$$C^{(0)} = h^*_{pp\sigma} h^*_{nn\delta} + h^*_{nn\sigma} h^*_{pp\delta}\,, \tag{32}$$

$$A^{(1)}_p = (1-\xi_N) + \xi_N \left(2m^*_p - m^*_n\right), \tag{33}$$

$$C^{(1)}_p = \xi_N h^*_{nn\delta}\,, \tag{34}$$

$$A^{(1)}_n = (1-\xi_N) + \xi_N \left(2m^*_n - m^*_p\right), \tag{35}$$

$$C^{(1)}_n = \xi_N h^*_{pp\delta}\,, \tag{36}$$

with $\xi_N \equiv 2\lambda_N$. The values of m^*_p and m^*_n should satisfy the energy minimization condition $\partial^2\mathcal{E}/\partial m^{*2}_p > 0$ and $\left(\partial^2\mathcal{E}/\partial m^{*2}_p\right)\left(\partial^2\mathcal{E}/\partial m^{*2}_n\right) - \left(\partial^2\mathcal{E}/\partial m^*_p \partial m^*_n\right)^2 > 0$.

Finally, the pressure P is given by

$$\begin{aligned} P &= \frac{1}{4}\left(E^*_{pF}\,\rho_{pB} - M^*_p\,\rho_{pS}\right) + \frac{1}{4}\left(E^*_{nF}\,\rho_{nB} - M^*_n\,\rho_{nS}\right) \\ &\quad - \frac{1}{2}M_N^2\left(\frac{m_\sigma}{g_{NN\sigma}}\right)^2\left(\frac{A^{(0)}}{C^{(0)}}\right)^2 - \frac{1}{2}M_N^2\left(\frac{m_\delta}{g_{NN\delta}}\right)^2\left(\frac{B^{(0)}}{C^{(0)}}\right)^2 \\ &\quad + \frac{1}{2}\left(\frac{g_{NN\omega}}{m_\omega}\right)^2\left(f_p\,h^*_{pp\omega} + f_n\,h^*_{nn\omega}\right)^2\rho_T^2 + \frac{1}{2}\left(\frac{g_{NN\rho}}{m_\rho}\right)^2\left(f_p\,h^*_{pp\rho} - f_n\,h^*_{nn\rho}\right)^2\rho_T^2\,, \end{aligned} \tag{37}$$

where $E^*_{p(n)F}$ is the Fermi energy of protons (neutrons).

3 Numerical analyses

For calculations of asymmetric matter, we have to determine the free meson-nucleon coupling constants. As seen in Eqs. (26), (28), (29) and (37), only the ratios to masses $(g_{NN\sigma}/m_\sigma)^2$ *etc.* are necessary. The isoscalar coupling constants are determined to reproduce the saturation properties of symmetric nuclear matter. (The saturation energy of $-15.75\,\mathrm{MeV}$ and the saturation density of $0.16\,\mathrm{fm}^{-3}$ are assumed.) The calculation has already been performed in Ref. [13] and $(g_{NN\sigma}/m_\sigma)^2 = 16.9\,\mathrm{fm}^2$ and $(g_{NN\omega}/m_\omega)^2 = 12.5\,\mathrm{fm}^2$ are obtained. The isovector coupling constants however cannot be determined uniquely [9]. Here we first fix the δ coupling constant by $(g_{NN\delta}/m_\delta)^2 = 1.0\,\mathrm{fm}^2$ (referred as the model 1) or $(g_{NN\delta}/m_\delta)^2 = 2.5\,\mathrm{fm}^2$ (referred as the model 2) and then determine the ρ coupling constant to reproduce the nuclear symmetry energy E_s. Although there still remains ambiguity in determining its value [15], we choose $E_s = 30.0\,\mathrm{MeV}$. The result is $(g_{NN\rho}/m_\rho)^2 = 1.727\,\mathrm{fm}^2$ for the model 1 or $(g_{NN\rho}/m_\rho)^2 = 2.855\,\mathrm{fm}^2$ for the model 2. The model 1 and 2 exhibit relatively weak and strong effect of the charge asymmetry respectively.

Then we calculate the properties of asymmetric nuclear matter. Figures 1(a) and 1(b) show the binding energies per nucleon $E \equiv \mathcal{E}/\rho_T - M_N$ in the models 1 and 2 as functions of the total baryon density ρ_T for several values of the asymmetry parameter

$a \equiv (\rho_{nB} - \rho_{pB})/\rho_T$. For increasing asymmetry, the saturation density shifts to lower values. Although there are little differences between Figs. 1(a) and 1(b), the model 2 produces somewhat lower saturation energies than the model 1. Especially for $a = 1$, the model 1 has no energy minimum whereas the model 2 exhibits a very shallow dip at $\rho_T \simeq 0.04\,\mathrm{fm}^{-3}$. In general the model 1 gives larger energies than the model 2 below the saturation density $\rho_T = 0.16\,\mathrm{fm}^{-3}$ of symmetric nuclear matter while the model 2 gives larger energies than the model 1 above the density. The difference between the two models becomes larger as the asymmetry parameter and the density increase.

The difference between the models 1 and 2 is explicitly seen in the density dependence of the symmetry energy. The binding energy per nucleon is a function of the total baryon density and the asymmetry parameter, and so is expanded as

$$E(\rho_T, a) = E(\rho_T, 0) + S_2(\rho_T)\, a^2 + S_4(\rho_T)\, a^4 + O\left(a^6\right). \tag{38}$$

The nuclear symmetry energy E_s mentioned above is the value of $S_2(\rho_T)$ at the saturation density of symmetric nuclear matter $\rho_T = 0.16\,\mathrm{fm}^{-3}$. Recently there are growing interests on the high-density behavior of $S_2(\rho_T)$ in conjunction with the numerical simulations of high-energy heavy-ion collisions [16-18]. Figure 2 shows S_2 and S_4 as functions of the total baryon density. The solid and dotted curves are the results of the models 1 and 2. Usually, $E(\rho_T, a)$ can be well expressed by up to the second term of Eq. (38). In fact S_4 is negligible to S_2. The symmetry energy S_2 increases almost linearly with density in both the models. The same feature is reproduced by the DBHF calculation [19]. We can see that the model 2 predicts slightly lower S_2 than the model 1 below $\rho_T = 0.16\,\mathrm{fm}^{-3}$ whereas, above the density, the model 2 predicts larger S_2 than the model 1. The difference becomes larger as the density increases

Next, we investigate the effective mass M_N^* of nucleons in asymmetric matter. Figure 3 shows M_p^* and M_n^* in the model 2 as functions of the density. The solid, dotted and dashed curves are the results using $a = 0.0$, 0.5 and 1.0 respectively. M_p^* becomes larger for increasing asymmetry parameter in the whole range of the density while M_n^* becomes lower. This is due to the isovector scalar mean-field $\langle \delta_3 \rangle$ in Eqs. (19) and (20). The difference between the results for $a = 0.0$ and $a = 0.5$ or between the results for $a = 0.5$ and $a = 1.0$ in M_n^* are much smaller than the corresponding differences in M_p^*. Furthermore Fig. 4 shows M_n^* (the solid curve) and M_p^* (the dashed curve) in the model 1 as functions of the asymmetry parameter at $\rho_T = 0.4\,\mathrm{fm}^{-3}$. M_p^* increases monotonically whereas M_n^* has a minimum at $a \approx 0.7$. Consequently, the difference between the two masses becomes larger as the asymmetry increases. The similar behavior can be found in the DBHF calculation [7].

The difference between the effective masses by the models 1 and 2 is shown in Fig. 5. The solid curve is for symmetric matter ($a = 0.0$). The dotted and dashed curves are the results by the models 1 and 2 for $a = 0.75$. The model 2 gives larger M_p^* and

lower M_n^* than the model 1 owing to stronger $NN\delta$ and $NN\rho$ coupling constants in the model 2. Furthermore Fig. 6 shows the effective masses as functions of the asymmetry parameter for several values of the densities. The solid and dotted curves are the results of the models 1 and 2. The differences between the two models become larger as the asymmetry increases.

In our model the renormalized coupling constants do not depend on whether the meson is scalar or vector, but are different for protons and for neutrons as seen from Eqs. (13) and (17). We then investigate the charge asymmetries of the effective interactions that are the essential difference of our model from the other relativistic mean-field models. Figures 7 and 8 show the density-dependences of the coupling constants in the model 2 for the isoscalar and isovector mesons, respectively. Part (a) is the result for protons and part (b) is for neutrons. The dotted and dashed curves are the results for $a = 0.5$ and $a = 1.0$. For a comparison we add the results of symmetric nuclear matter by the solid curves in Fig. 7. In general the coupling constants decrease monotonically as the density increases. The $pp\sigma(\omega)$ coupling becomes stronger but the $nn\sigma(\omega)$ coupling becomes weaker for larger asymmetry parameter. The difference between the results for $a = 0.0$ and $a = 0.5$ or between the results for $a = 0.5$ and $a = 1.0$ in Fig. 7(b) is much smaller than the corresponding difference in Fig. 7(a). On the contrary, the $pp\delta(\rho)$ coupling becomes weaker but the $nn\delta(\rho)$ coupling becomes stronger for larger asymmetry. The difference between the results for $a = 0.5$ and $a = 1.0$ in Fig 8(b) is nearly the same as the corresponding difference in Fig. 8(a). These facts explicitly reveal the charge-asymmetric features of the renormalized effective coupling constants in our model.

The differences between the coupling constants by the models 1 and 2 are shown in Figs. 9 and 10. The solid curve is for symmetric matter ($a = 0.0$). The dotted and dashed curves are the results by the models 1 and 2 for $a = 0.75$. The model 2 gives stronger $pp\sigma(\omega)$ coupling and weaker $nn\sigma(\omega)$ coupling than the model 1. On the contrary, the model 1 gives stronger $pp\delta(\rho)$ coupling and weaker $nn\delta(\rho)$ coupling than the model 2. Furthermore Figs. 11(a) and (b) show $NN\sigma(\omega)$ and $NN\delta(\rho)$ coupling constants at $\rho_T = 0.4\,\mathrm{fm}^{-3}$ as functions of the asymmetry parameter. The thick (thin) solid and dotted curves are the results for protons and neutrons in the model 1 (2). We can clearly see the charge asymmetry of the effective coupling constants and the differences between the models 1 and 2.

Finally, we apply our model to the cold neutrino-free non-rotating dense neutron star matter containing only nucleons as baryons and electrons and muons as leptons. In this case, the asymmetry parameter a or proton fraction $f_p = (1-a)/2$ is determined by β-equilibrium condition under the charge neutrality [19],

$$f_p\,\rho_T = \frac{1}{3\pi^2}\left[\,\mu_e^3 + \theta\left(\mu_e - m_\mu\right)\left(\mu_e^2 - m_\mu^2\right)^{3/2}\right], \tag{39}$$

where m_μ is muon mass and μ_e is the chemical potential of electrons given by the sym-

metry energies in Eq. (38);

$$\mu_e = 4a\left(S_2 + 2S_4\, a^2\right). \tag{40}$$

Equations (28), (29) and (39) should be solved self-consistently. The resulting proton fraction f_p is shown in Fig. 12. The solid and dashed curves are the results of the models 1 and 2. Below the nuclear matter saturation density $\rho_T = 0.16\,\mathrm{fm}^{-3}$, the model 2 predicts slightly smaller f_p than the model 1 whereas the model 2 becomes larger than the model 1 as the density increases above the saturation. This behavior of the difference between the two models just reflects the density-dependence of the symmetry energy S_2 in Fig. 2. In addition we calculate $\triangle E \equiv E(\rho_T, a) - E(\rho_T, 0)$ in Fig. 13. The model 2 predicts larger S_2, as seen in Fig. 2, but lower $\triangle E$ than the model 1 at higher densities. This is due to the larger proton fraction f_p or the lower asymmetry parameter a of the model 2 in Fig. 12. At higher densities, the effect of a^2 overcomes the effect of S_2.

The properties of the neutron stars are calculated by integrating the so-called Tolman-Oppenheimer-Volkov (TOV) equation [20]. For this purpose, we need the equation of state (EOS). We assume that the EOS of our model describes the core region $\left(\rho_T \geq 0.08\,\mathrm{fm}^{-3}\right)$ of neutron stars. For the outer region $\left(\rho_T < 0.08\,\mathrm{fm}^{-3}\right)$, we use the EOS by Feynman-Metropolis-Teller, Baym-Pethick-Sutherland and Negele-Vautherin (NV) from Ref. [21]. Figure 14 shows the EOS by the model 1. It is found that our EOS is similar to the DBHF calculation [22].

Figures 15 and 16 show the gravitational mass of a neutron star in units of the solar mass as functions of the central energy density $\mathcal{E}_C$ and radius R. The solid and dotted curves are the results of the models 1 and 2. They exhibit the general feature of the stiff EOS [23] that predicts both a large maximum mass and a large radius. The maximum mass by the model 1 is $M = 2.19\,M_\odot$ at $\mathcal{E}_C = 2.08 \times 10^{15}\mathrm{g/cm}^3$ and $R = 11.8\,\mathrm{km}$ while the model 2 predicts $M = 2.21 M_\odot$ at $\mathcal{E}_C = 2.01 \times 10^{15}\mathrm{g/cm}^3$ and $R = 12.0\,\mathrm{km}$. So as to understand the differences between the results of the two models, Fig. 17 shows the EOS again in the different units and scale from Fig. 14. The triangle-solid and cross-dotted curves are the results by the model 1 and 2 respectively. The circle-dashed curve is the EOS by NV. The EOS by the model 2 becomes softer than the EOS by the model 1 below the intersection $\left(\rho_T = 0.08\,\mathrm{fm}^{-3}\right)$ with the NV EOS, while the former becomes slightly stiffer than the latter above the intersection. Therefore the model 2 in Figs. 15 and 16 exhibit the feature of stiffer EOS than the model 1.

4 Summary and conclusions

The fully consistent theory of asymmetric nuclear matter should satisfy the charge-asymmetry of the densities, effective masses and effective interactions of protons and neutrons simultaneously. The DBHF theory satisfies such a full consistency whereas there have been no corresponding relativistic mean-field theories even now. The present

work is a resolution of this problem.

We have extended the ZM model to asymmetric matter based on the constituent quark picture of nucleons. The effects of scalar mean-fields on all the three constituent quarks in medium have been taken into account. They produce the medium corrections to the meson-nucleon coupling constants or the renormalized effective interactions. Since the renormalizations depend on the effective masses of nucleons, both the effective masses and coupling constants have to be determined self-consistently. Including the isovector scalar mean-field by $\delta[a_0(980)]$ meson, the masses of protons and neutrons are different from each other. Therefore the renormalized coupling constants for protons are different from those for neutrons. Consequently, we have fully consistent relativistic mean-field model of asymmetric matter containing charge-asymmetric effective interactions as the DBHF theory.

We have numerically investigated our model in detail and explicitly revealed its charge-asymmetric nature. Then the model is applied to the cold β-stable neutron star matter. The results exhibit the general features of a stiff EOS. In several aspects of these calculations, the similar results to the DBHF calculations have been found. In this respect we want to emphasize that our model is not a simplified effective version of the complicated DBHF theory as the works in Refs. [5,6], but is an independent theory.

The reliability and applicability of our model has to be investigated further. For an example the surface region or the neutron skin of largely neutron-rich nuclei may be a candidate of highly charge-asymmetric medium. It is however not appropriate to our purpose since the relevant density is rather low. So as to clear the effects of the charge-asymmetric interactions, both the high density and high asymmetry are necessary. Therefore the neutron star is a good subject of our investigation. The present study is however insufficient because of the important roles of hyperons in neutron stars [23]. In our picture the effective interactions between two hyperons and between nucleons and hyperons will be also charge-asymmetric. We will investigate their effects in future works.

References

[1] B.D. Serot and J. D. Walecka, *Advances in Nuclear Physics*, Vol.**16** (Plenum, New York, 1986).

[2] B. ter Harr and R. Malfliet, Phys. Rev. Lett. **59** (1987) 1652.

[3] L. Engvik, G. Bao, M. Hjorth-Jensen, E. Osnes and E. Østgaard, Astrophys. J. **469** (1996) 794.

[4] F. de Jong and H. Lenske, Phys. Rev. **C57** (1998) 3099, [arXiv:mucl-th/9707017].

[5] F. Hoffman, C.M. Keil and H. Lenske, Phys. Rev. **C64** (2001) 034314, [arXiv:nucl-th/0007050].

[6] J. K. Bunta and Š. Gmuca, arXiv:nucl-th/0309046.

[7] S. Ulrych and H. Můther, Phys. Rev. **C56** (1997) 1788, [arXiv:nucl-th/9706030].

[8] J. Zimanyi and S.A. Moszkowski, Phys. Rev. **C42** (1990) 1416. It is noted that the NLW model has linear meson-baryon couplings in spite of its name. On the contrary, the ZM model is true nonlinear mean-field model.

[9] S. Kubis and M. Kutschera, Phys. Lett. **B399** (1997) 191, [arXiv:astro-ph/9703049].

[10] B. Liu, V. Greco, V. Baran, M. Colonna and M.Di Toro, Phys. Rev. **C65** (2002) 045201, [arXiv:nucl-th/0112034].

[11] A.R. Taurines, C.A.Z. Vasconcellos, M. Malheiro and M. Chiapparini, Phys. Rev. **C63** (2001) 065801, [arXiv:nucl-th/0010084].

[12] R. Aguirre and A.L.De Paoli, Eur. Phys. J. **A13** (2002) 501, [arXiv:nucl-th/0102029].

[13] K. Miyazaki, CERN Document Server (CDS) ext-2003-062 revised by Mathematical Physics Preprint Archive (mp_arc) 05-178.

[14] K. Miyazaki, CERN Document Server (CDS) ext-2002-056 revised by Mathematical Physics Preprint Archive (mp_arc) 05-141.

[15] J.M. Pearson and R.C. Nayak, Nucl. Phys.**A668** (2000) 163.

[16] Bao-An Li, Nucl. Phys. **A708** (2002) 365, [arXiv:nucl-th/0206053].

[17] L.-W. Chen, V. Greco, C.M. Ko and B.-A. Li, Phys. Rev. Lett **90** (2003) 162701, [arXiv:nucl-th/0211002].

[18] V. Greco, V. Baran, M. Colonna, M.Di Toro, T. Gaitanos and H.H. Wolter, Phys. Lett. **B562** (2003) 215, [arXiv:nucl-th/0212102].

[19] C.-H. Lee, T.T.S. Kuo, G.Q. Li and G.E. Brown, arXiv:nucl-th/9703034.

[20] W.D. Arnett and R.L. Bowers, Astrophys. J. Suppl. **33** (1977) 415.

[21] V. Canuto, Ann. Rev. Astr. Ap. **12** (1974) 167; **13** (1975) 335.

[22] F. Weber, J. Phys. **G27** (2001) 465, [arXiv:astro-ph/0008376].

[23] S. Balberg, I. Lichtenstadt and G.B. Cook, Astrophys. J. Suppl. **121** (1999) 515.

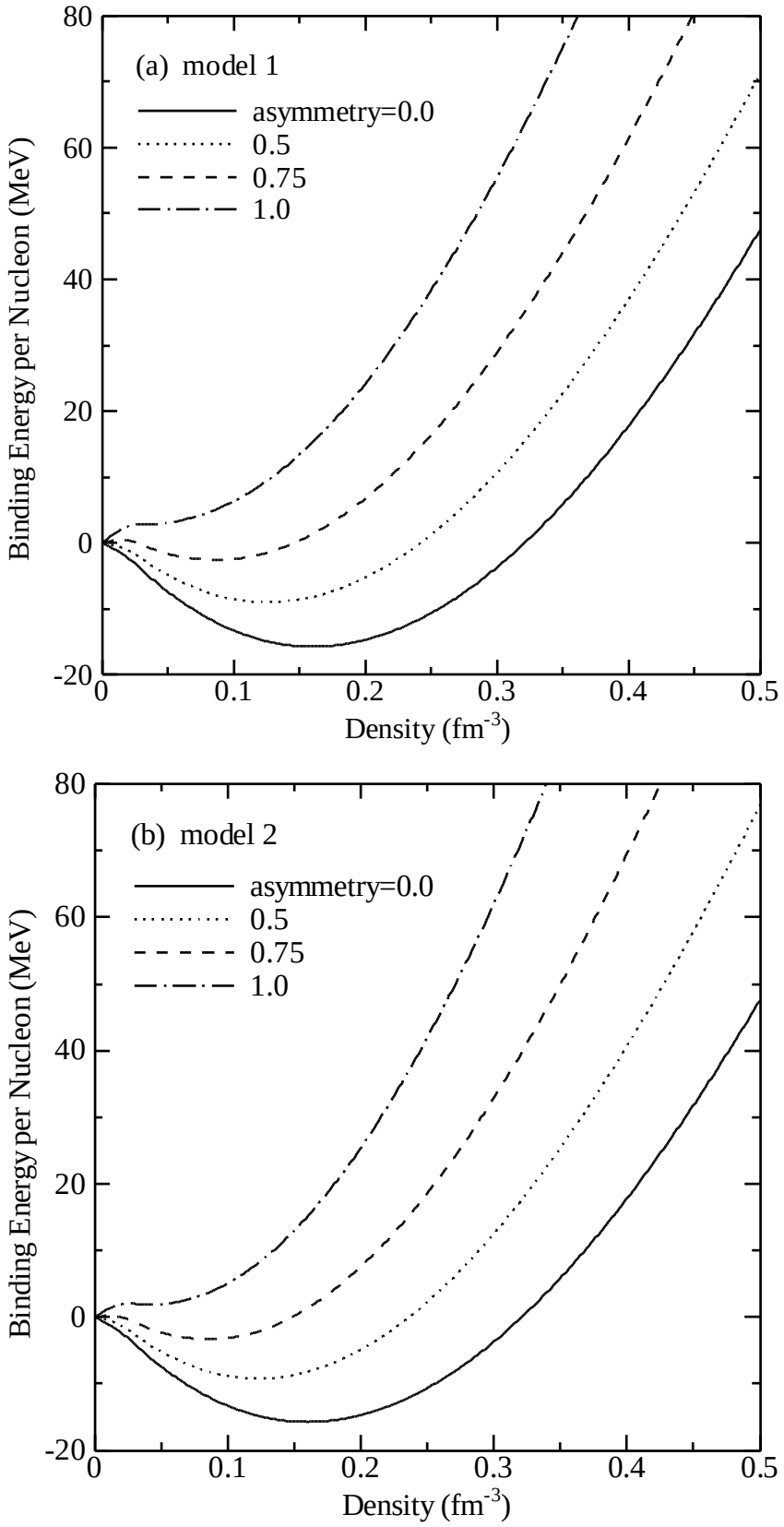

Figure 1: The binding energies per nucleon calculated by (a) the modesl 1 and (b) the model 2 as functions of the total baryon density. The solid, dotted, dashed and dotted-dashed curves are the results using the asymmetry parameter $a = 0.0$, 0.5, 0.75 and 1.0 respectively.

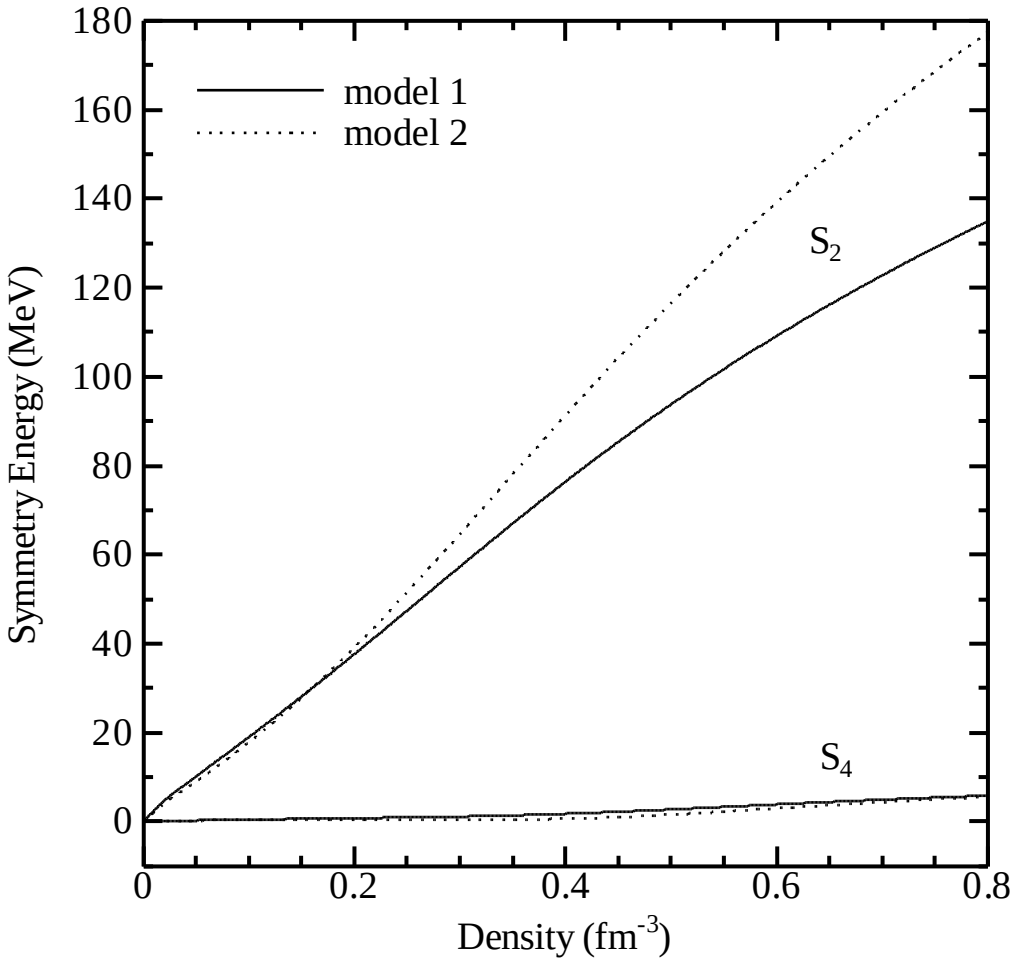

Figure 2: The symmetry energies defined in Eq. (38) as functions of the total baryon density. The solid and dotted curves are the results by the models 1 and 2.

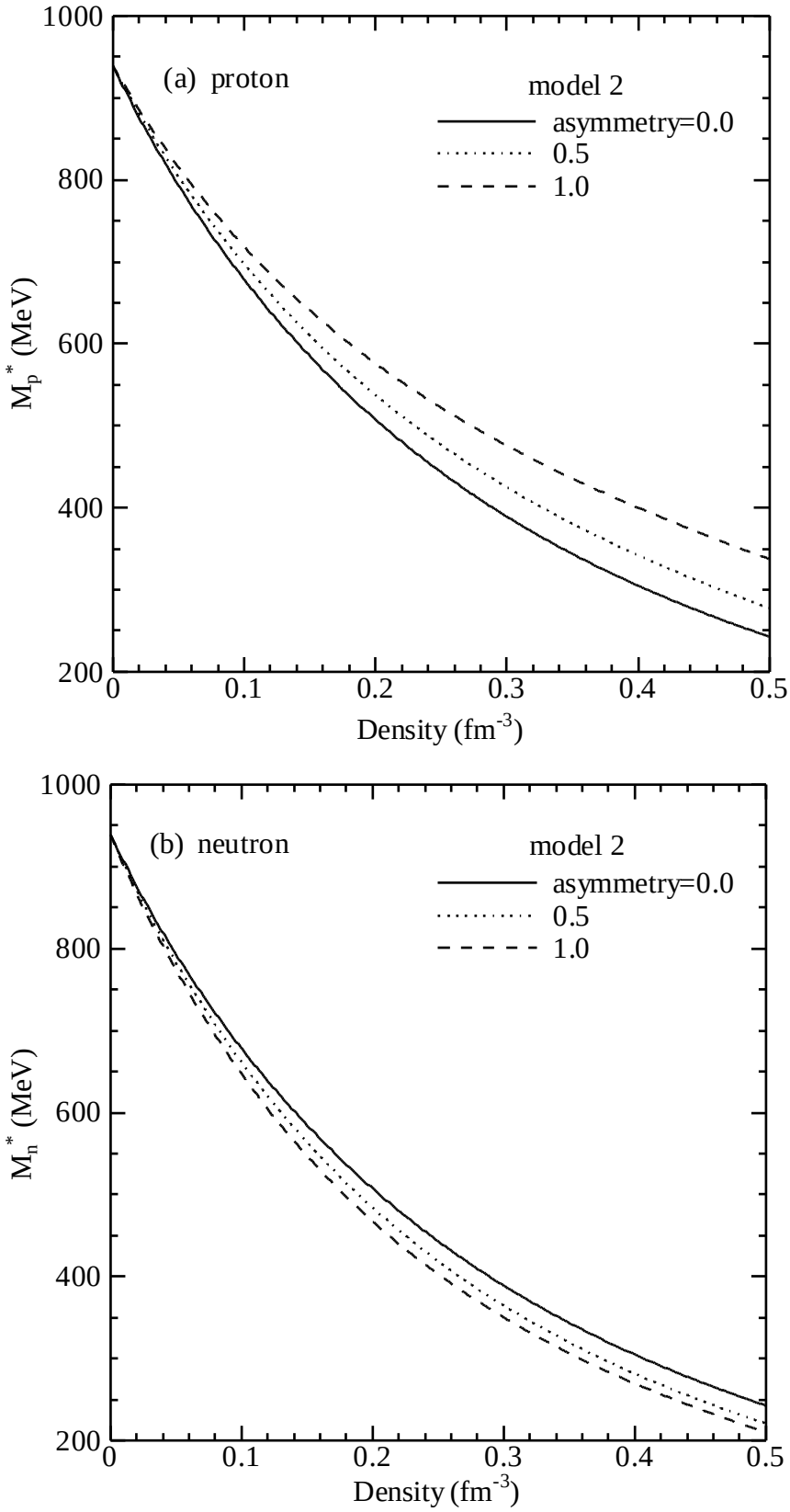

Figure 3: The relativistic effective masses of (a) protons and (b) neutrons calculated by the model 2 as functions of the total baryon density. The solid, dotted and dashed curves are the results using the asymmetry parameter $a = 0.0$ (symmetric nuclear matter), 0.5 and 1.0 (pure neutron matter).

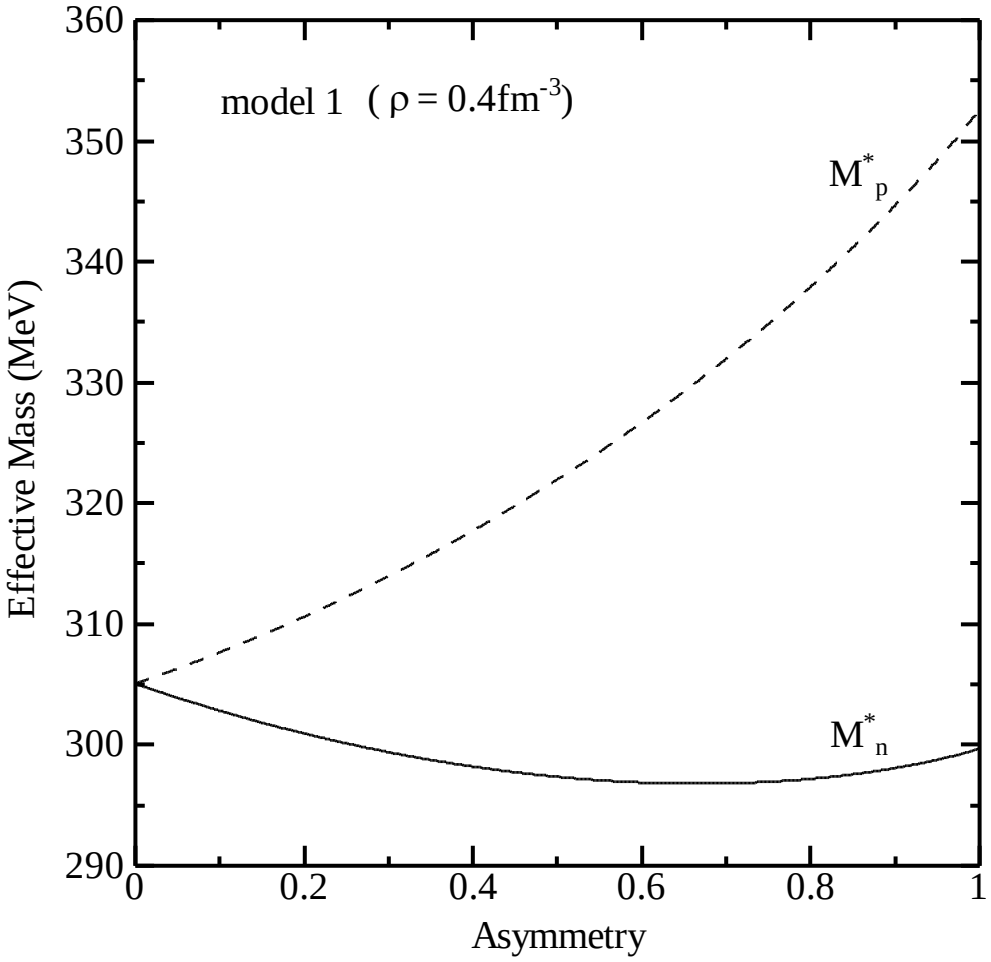

Figure 4: The relativistic effective masses of neutrons (the solid curve) and protons (the dashed curve) as functions of the asymmetry parameter calculated by the model 1 at the total baryon density $0.4\,\mathrm{fm}^{-3}$.

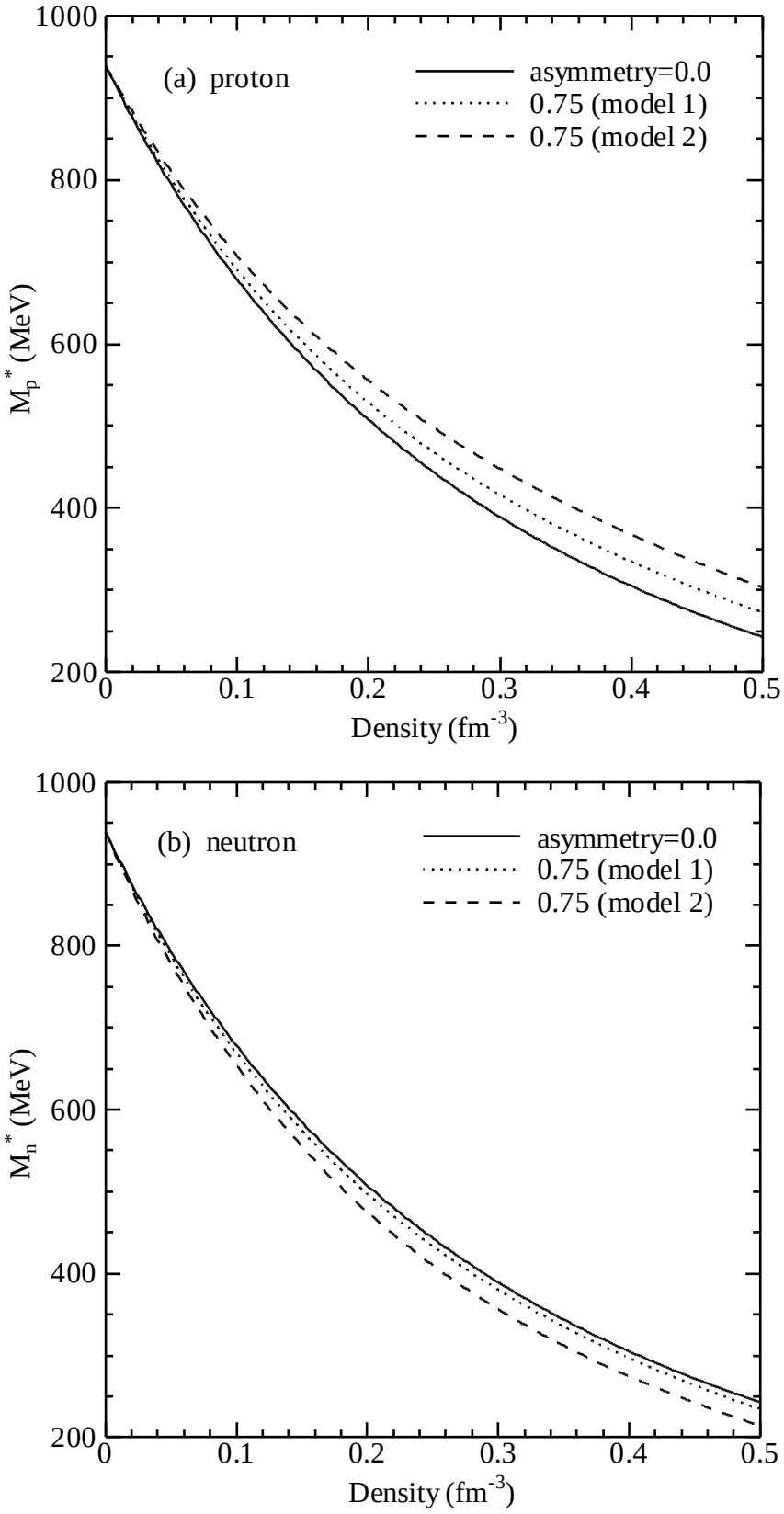

Figure 5: The relativistic effective masses of (a) protons and (b) neutrons as functions of the total baryon density. The solid curve is the result for symmetric matter. The dotted and dashed curves are the results for the asymmetry parameter $a = 0.75$ calculated by the model 1 and 2 respectively.

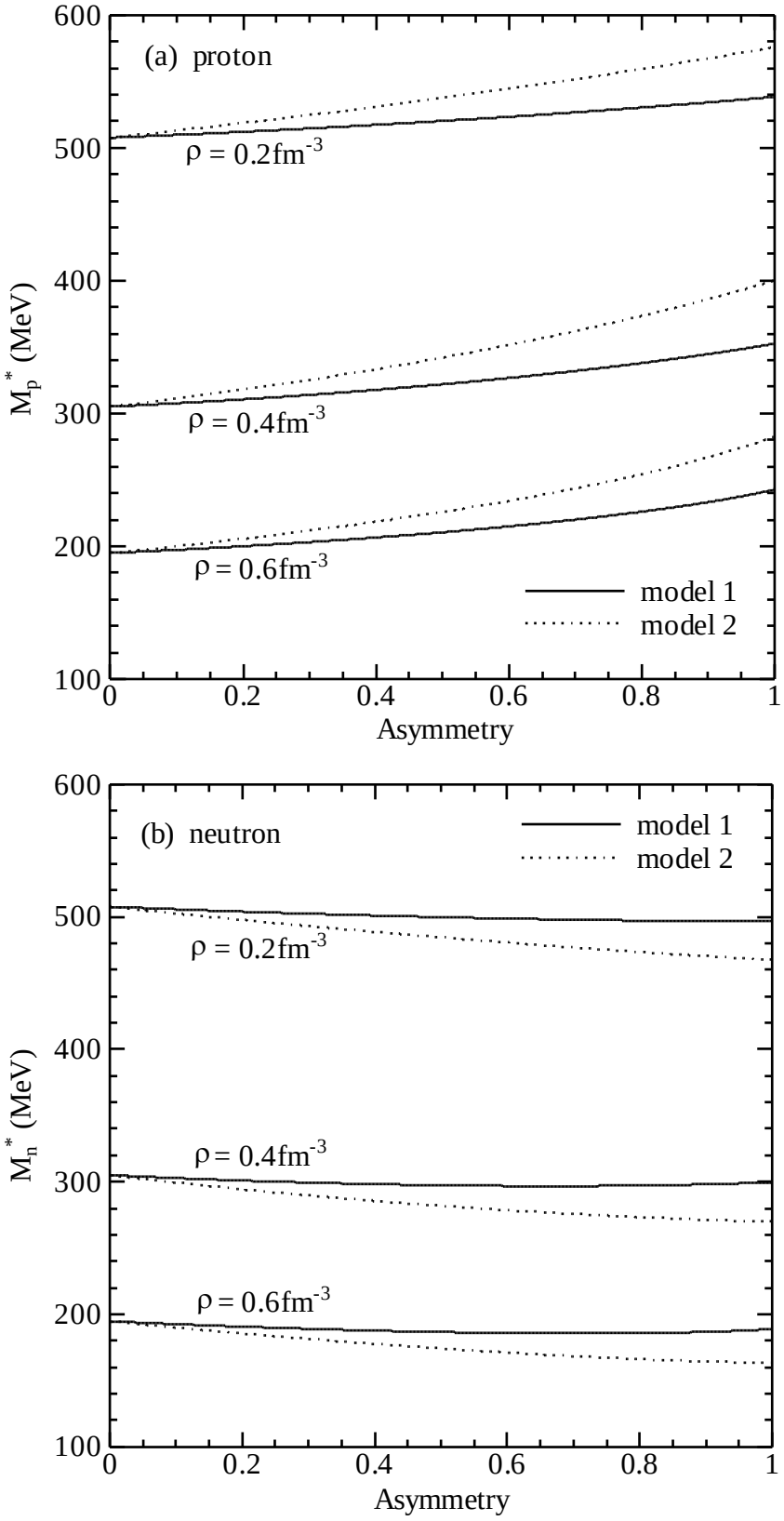

Figure 6: The relativistic effective masses of (a) protons and (b) neutrons as functions of the asymmetry parameter at the total baryon densities 0.2fm^{-3}, 0.4fm^{-3} and 0.6fm^{-3}. The solid and dotted curves are the results by the models 1 and 2.

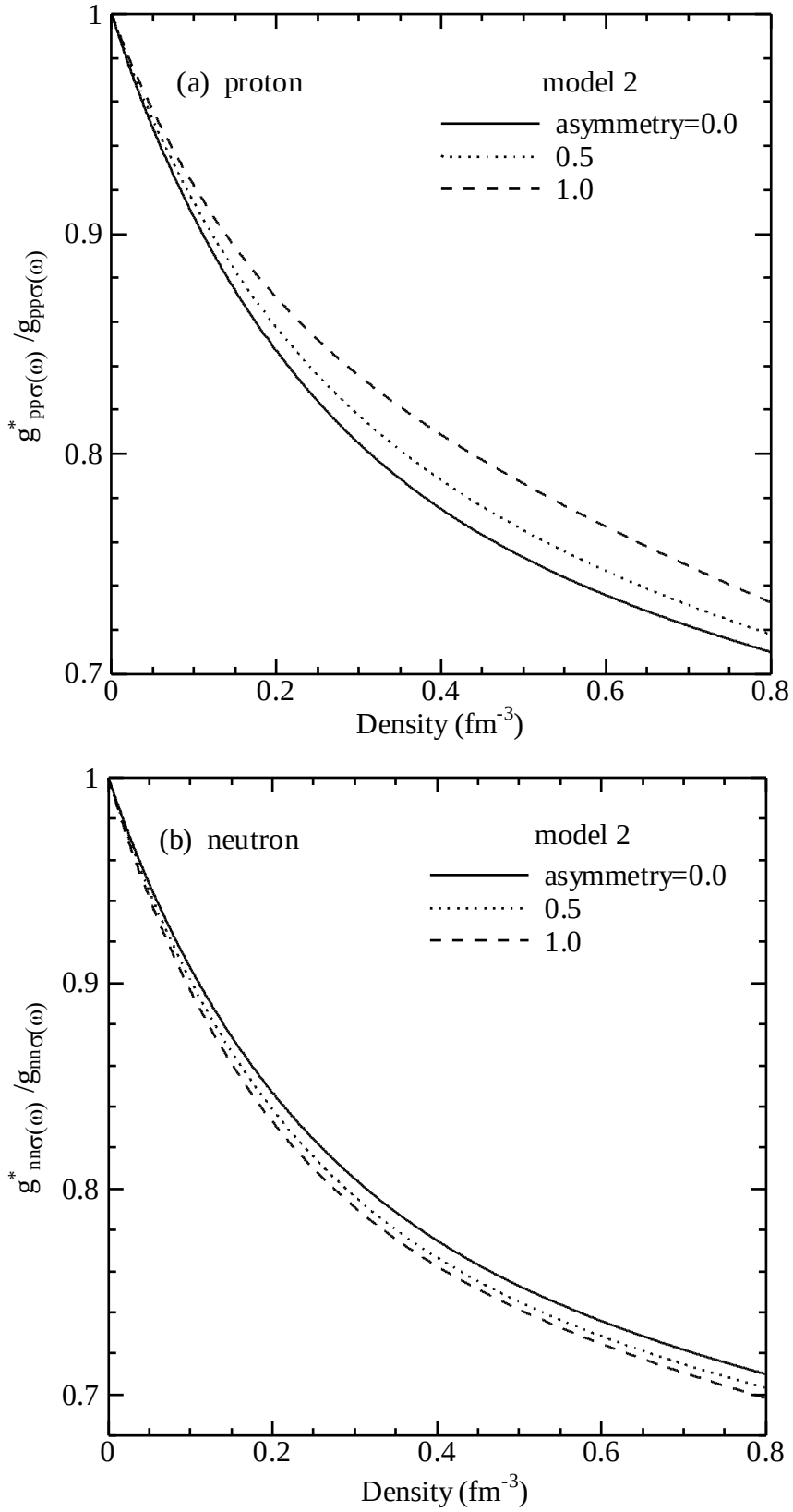

Figure 7: The renormalized (a) $pp\sigma(\omega)$ and (b) $nn\sigma(\omega)$ coupling constants calculated by the model 2 as functions of the total baryon density. The solid, dotted and dashed curves are the results using the asymmetry parameter $a = 0.0$ (symmetric nuclear matter), 0.5 and 1.0 (pure neutron matter).

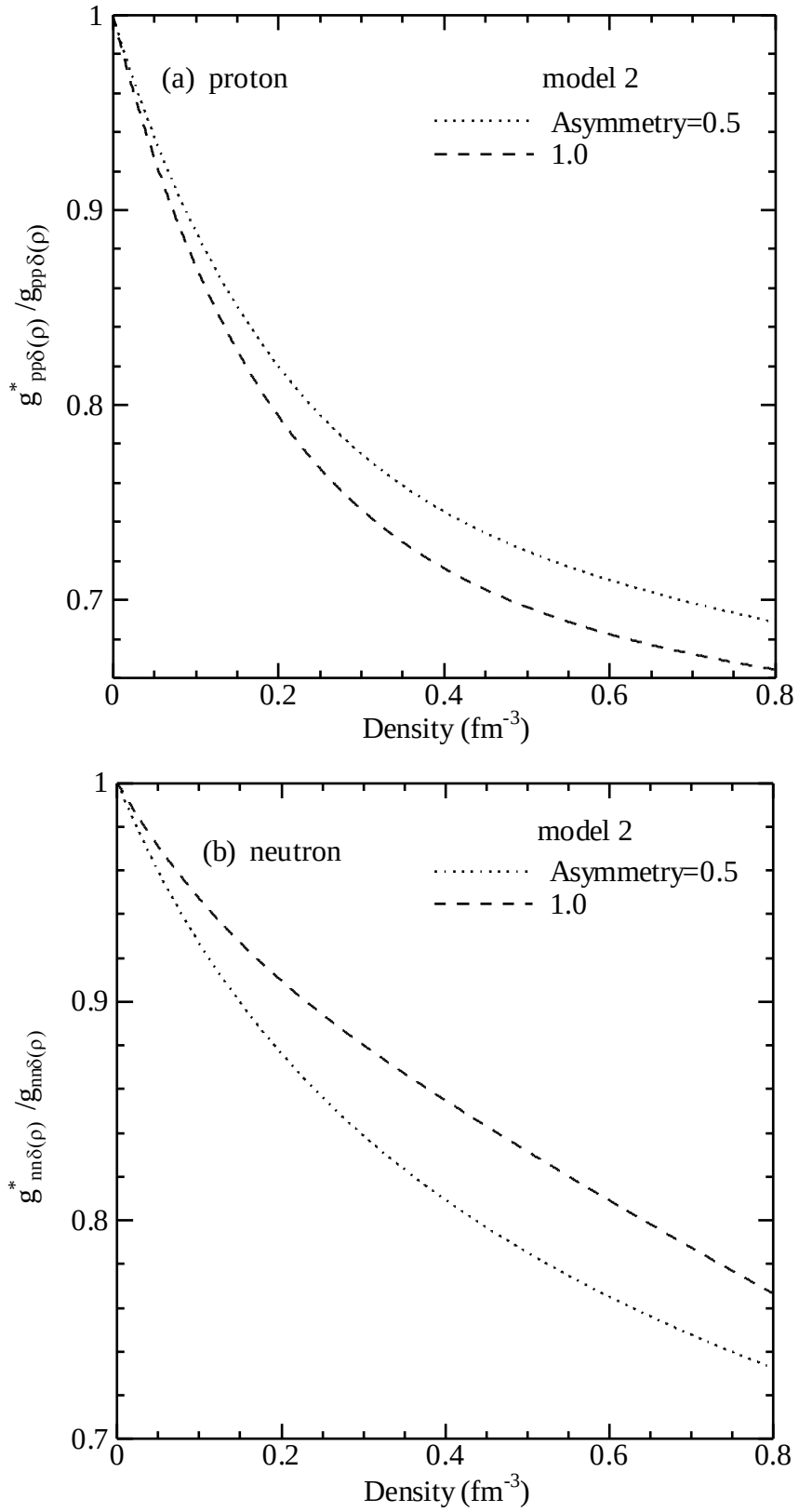

Figure 8: The renormalized (a) $pp\delta(\rho)$ and (b) $nn\delta(\rho)$ coupling constants calculated by the model 2 as functions of the total baryon density. The dotted and dashed curves are the results using the asymmetry parameter $a = 0.5$ and 1.0 (pure neutron matter).

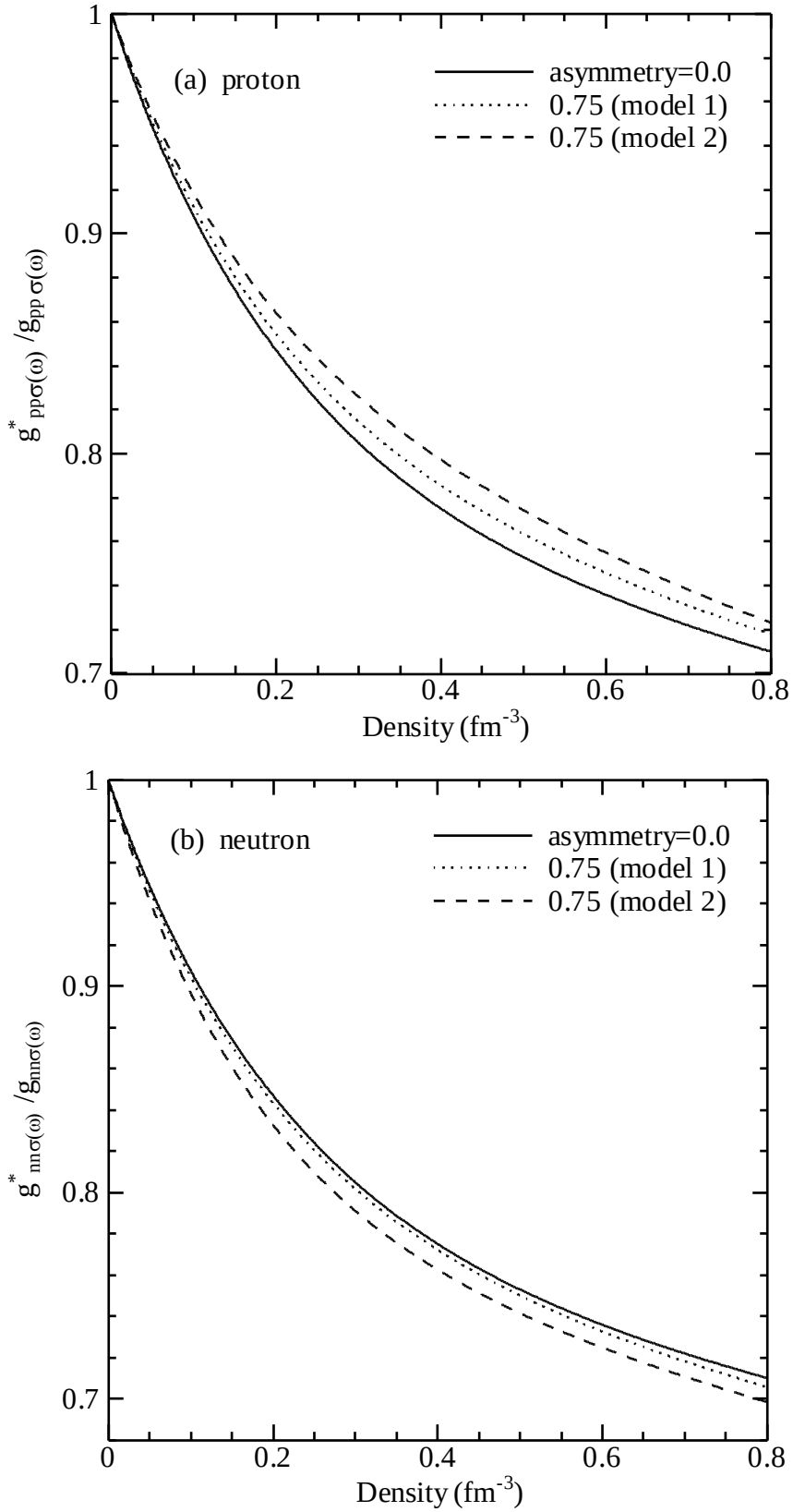

Figure 9: The renormalized (a) $pp\sigma(\omega)$ and (b) $nn\sigma(\omega)$ coupling constants calculated as functions of the total baryon density. The solid curve is the result for the symmetric matter. The dotted and dashed curves are the results for the asymmetry parameter $a = 0.75$ calculated using the models 1 and 2.

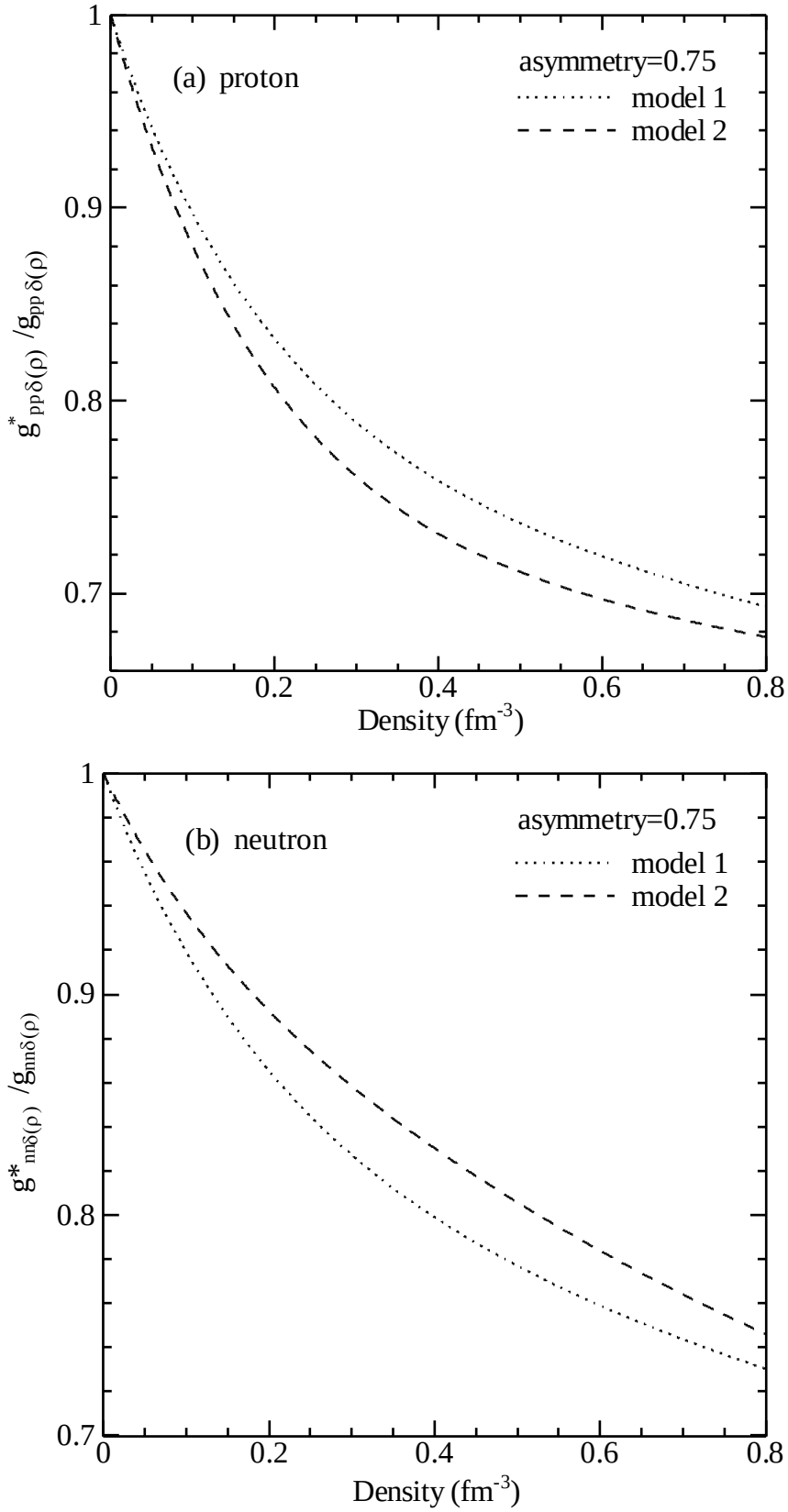

Figure 10: The renormalized (a) $pp\delta(\rho)$ and (b) $nn\delta(\rho)$ coupling constants calculated as functions of the total baryon density. The dotted and dashed curves are the results for the asymmetry parameter $a = 0.75$ calculated using the models 1 and 2.

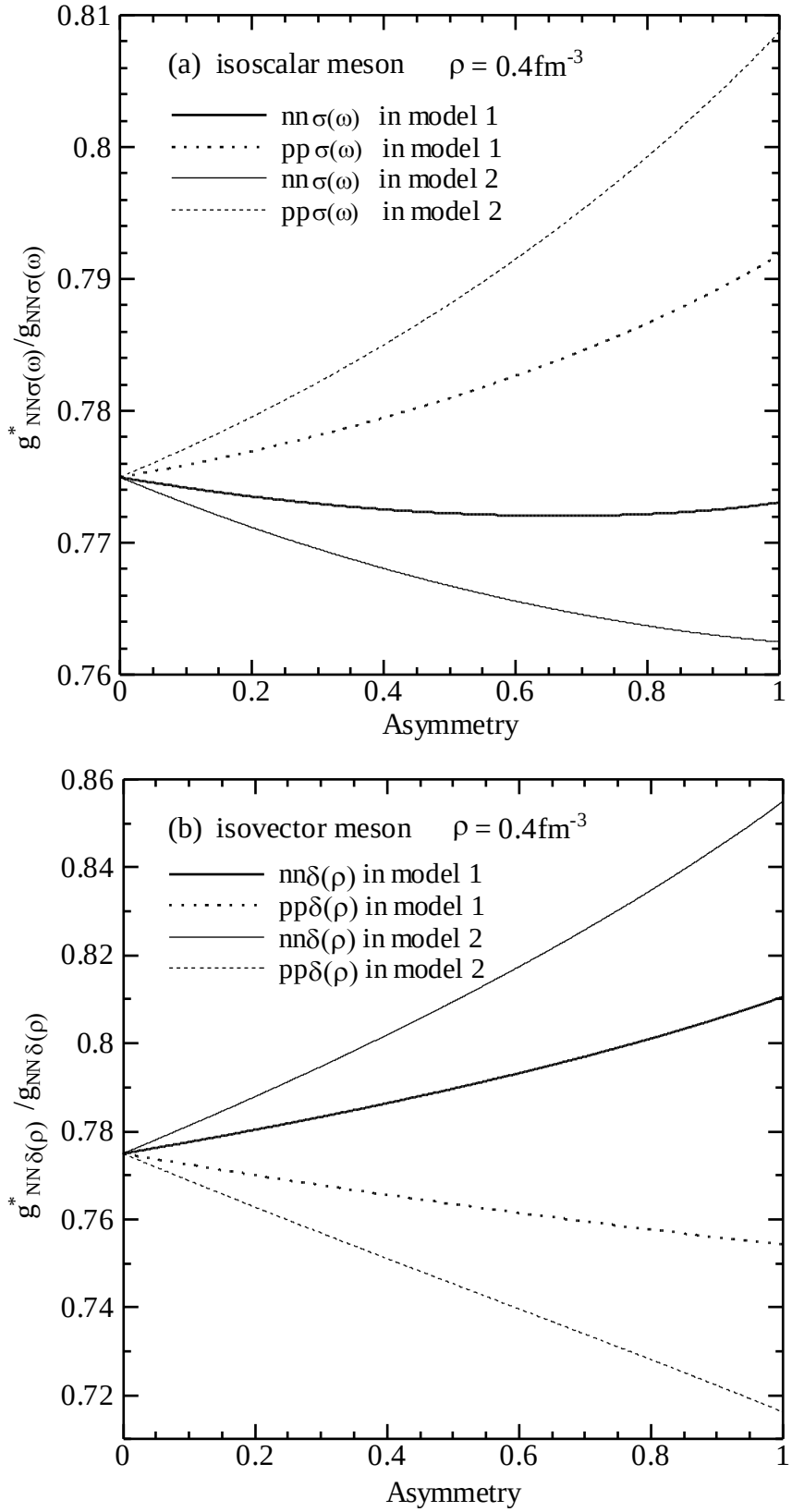

Figure 11: The renormalized (a) $NN\sigma(\omega)$ and (b) $NN\delta(\rho)$ coupling constants at the total baryon density 0.4fm^{-3} as functions of the asymmetry parameter. The solid and dotted curves are for protons and neutrons respectively. The thick and thin curves are calculated by using the models 1 and 2.

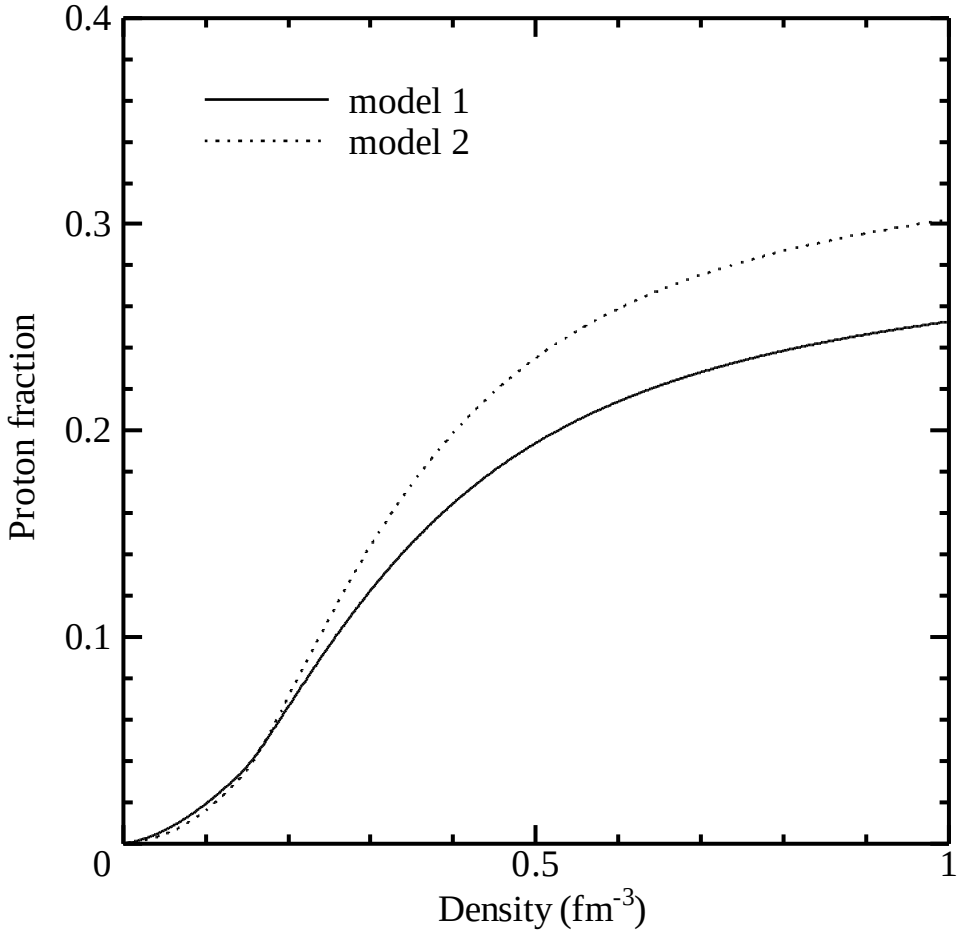

Figure 12: The proton fractions as functions of the total baryon density under β-equilibrium. The solid and dotted curves are calculated by using the models 1 and 2.

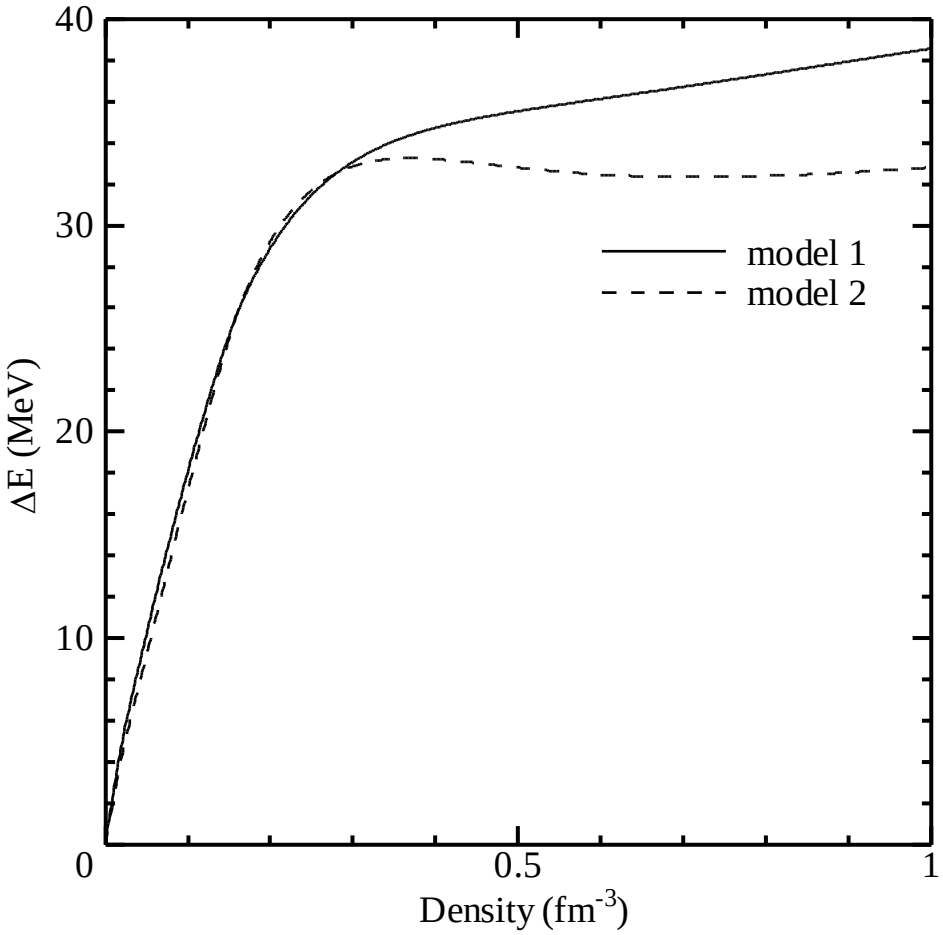

Figure 13: The differences between the energy density of asymmetric matter under β-equilibrium and that of symmetric matter, as functions of the total baryon density. The solid and dashed curves are calculated by using the models 1and 2.

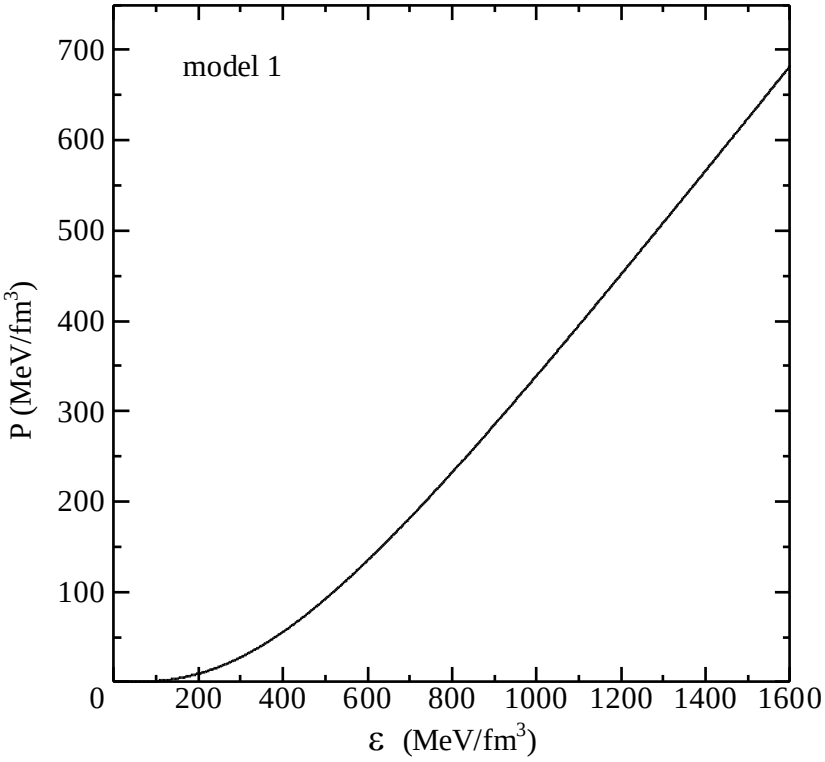

Figure 14: The equation-of-state calculated using the model 1.

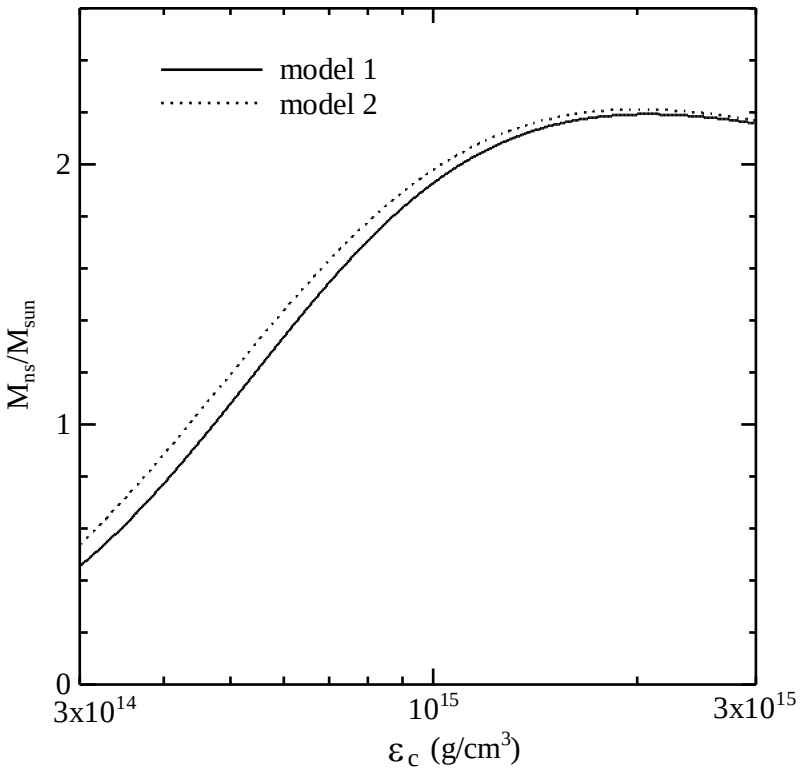

Figure 15: The neutron star masses in units of the solar mass as functions of the central energy density. The solid and dotted curves are the results of the models 1 and 2

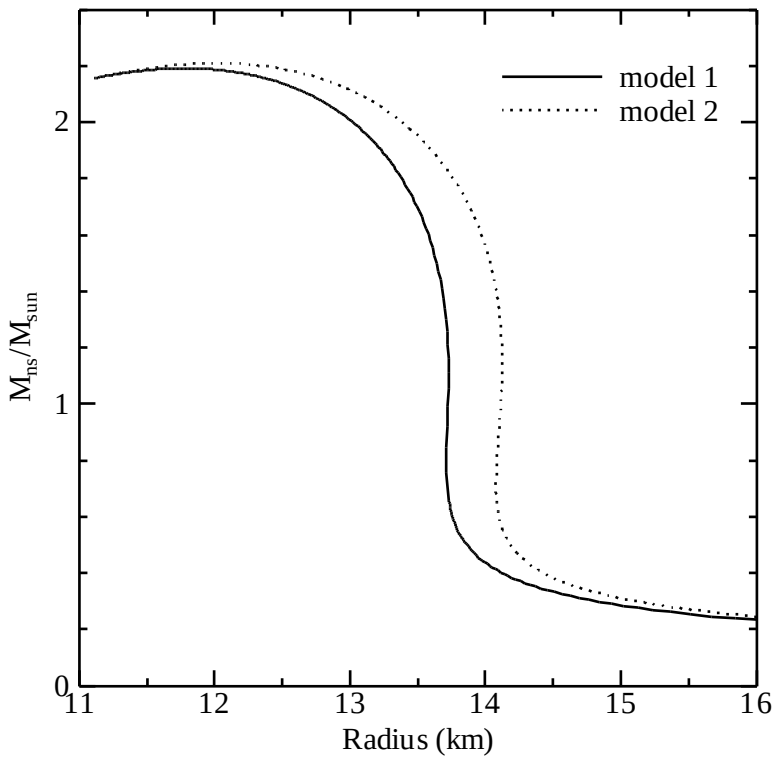

Figure 16: The neutron star masses in units of the solar mass versus the neutron star radius. The solid and dotted curves are the results of the models 1 and 2.

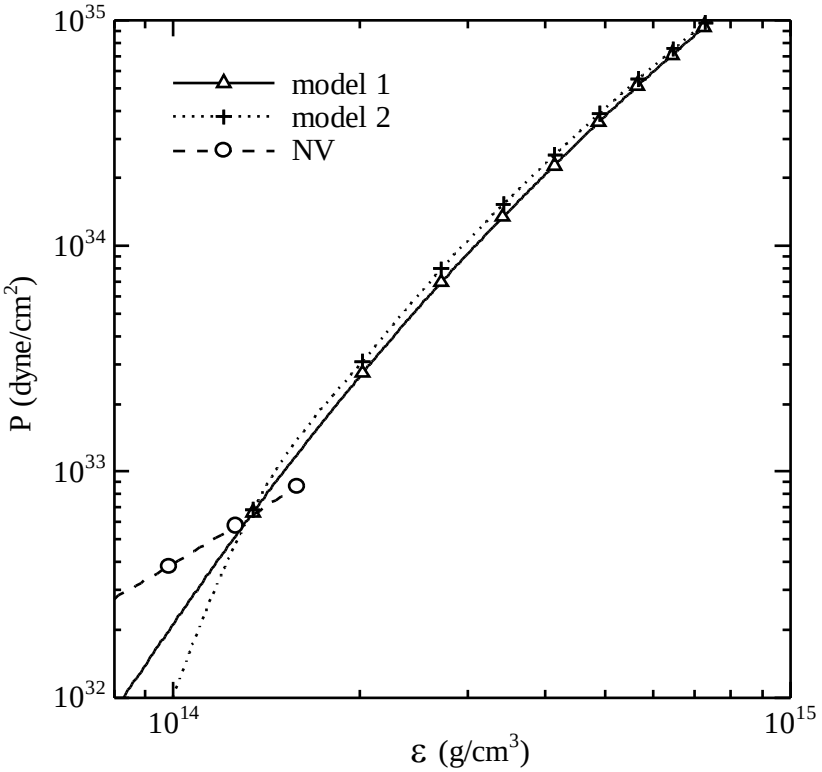

Figure 17: The equation-of-state by the model 1 (the solid curve) and by the model 2 (the dotted curve). The dashed curve is due to Negele-Vautherin.